Nuclear Instruments and Methods in Physics Research B40/41 (1989) 104–107
North-Holland, Amsterdam

IONIZATION OF HELIUM BY PROTONS, ELECTRONS, AND THEIR ANTIPARTICLES: DYNAMICAL EFFECTS OF PROJECTILE MASS AND CHARGE IN ANGULAR-DIFFERENTIAL CROSS SECTIONS

T.J. GAY and R.E. OLSON

Physics Department, University of Missouri-Rolla, Rolla, Missouri 65401 USA

We present classical trajectory Monte Carlo calculations of differential cross sections for direct ionization (without charge transfer) of He by protons, electrons, and their antiparticles at 200 keV/amu. Dynamical effects depending on the charge-sign and mass of the projectiles, as elucidated by the calculations, are discussed, and an experiment to test some of the calculations with antimatter projectiles is proposed.

In this paper, we consider some dynamical aspects of single ionization in He collisions with protons, electrons, and their antiparticles. We discuss only simple direct ionization, in which the electron removed from the He target is placed in a continuum state, and the remaining He^+ ion is not excited, i.e.,

$$x + He(1s^2) \rightarrow x + He^+(1s) + e^-, \qquad (1)$$

where $x = (p, \bar{p}, e^+, e^-)$. In the Bethe–Born approximation [1], differential and (consequently) total cross sections for any collision process depend neither on the projectile mass nor on the sign of its charge. Differences between cross sections for p, $\bar{p}$, e^+, and e^- projectiles are thus unambiguous evidence for deviation from this simple physical picture.

Recent developments in experimental technology have made possible the measurement of total cross sections for a variety of collisions involving positrons and antiprotons [2–5]. Considering reaction (1) at 1 MeV/amu incident energy, for example, we find total cross sections, in units of 10^{-17} cm^2, of 2.1(2), 2.0(1), 2.1(1), and 2.0(2) for protons [6], antiprotons [2], positrons [3], and electrons [7], respectively. Significant departures from the Bethe–Born theory begin to appear at lower energies, as would be expected. The same cross sections at 200 keV/amu are 7.2(7), 4.5(2), and 3.7(4) for protons, positrons, and electrons ($\bar{p}$ measurements have not been made below 0.5 MeV). An obvious question is: what dynamical effects cause the differences in total cross sections as the projective energy is decreased? One can expect to find at least a partial answer in a more detailed experimental investigation – the measurement of electron ejection cross sections for reaction (1), differential in angle and/or energy of ejection.

We report here differential cross sections calculated using the classical trajectory Monte Carlo (CTMC) method [8,9]. These calculations have been made fo collision (1) at an incident energy of 200 keV/am (corresponding to 109 eV electrons and positrons), be cause of the large amount of data available for proton and electrons at this velocity with which we can com pare our results. Good qualitative agreement betwee our calculations and these data lends credence to ou predictions for $\bar{p}$ and e^+ scattering, which have not ye been investigated with differential measurements.

The CTMC method is a completely classica technique which inherently includes the interaction o the electrons with both the target nucleus and projectil the effect of target recoil and, in the case of positive charged projectiles, electron capture. Perhaps most im portantly, it considers the ionization and charge-trans fer channels in a complete, consistent fashion. The H target is described using the independent electron mod [10], with an effective charge and binding energy o 1.6875 and 0.903 a.u. respectively.

Our calculations of total cross sections yield value of 6.6(2), 5.2(2), and $4.5(2) \times 10^{-17}$ cm^2 for proton positrons, and electrons, respectively, in reasonab agreement with the experimental values. (Our calcul tion for the $\bar{p}$ total cross section is $4.9(2) \times 10^{-17}$ cm^2 The relatively large difference between the p and e cross sections is seen, from consideration of other rea tion channels, to be due to the fact that while bot positrons and protons remove about the same numb of electrons from the target, a factor-of-four great fraction of these are captured by positrons than b protons; the higher positronium formation cross sectio means that "free" electron flux associated with dire ionization (1) is reduced in the positron case. This ca be understood as a mass effect; the positron's muc lower momentum makes velocity-vector matching wi a target electron, the precursor of a capture event, mo likely.

0168-583X/89/$03.50

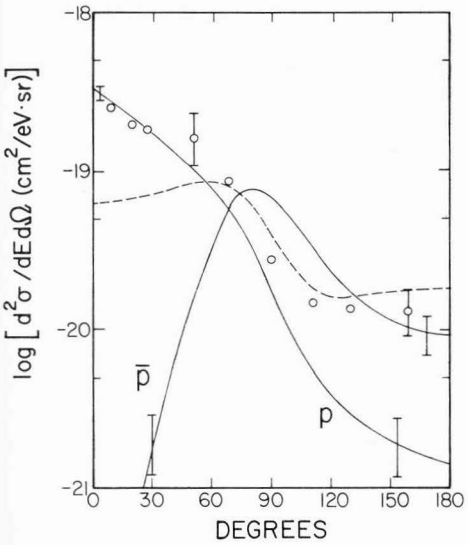

Fig. 1. Doubly-differential cross sections for direct ionization of He by protons and antiprotons at 200 keV/amu. Electron ejection energy = 27.2 eV. Solid lines are CTMC calculations; dashed line is the first Born calculation of ref. [15]. Vertical bars on CTMC curves represent statistical error of the calculation. Proton data of ref. [16] are shown by open circles; representative error bars are indicated.

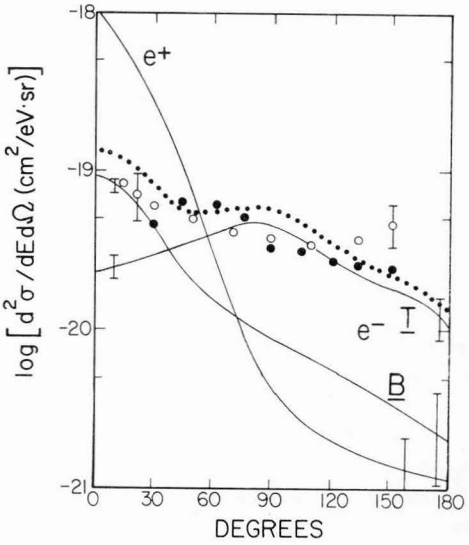

Fig. 3. Double-differential cross sections for electron emission at 27.2 eV in ionization of He by electrons and positrons of energy 109 eV. For incident electrons, contributions from the beam are labeled B, and target contributions are labeled T. The dotted line represents the sum of target and beam contributions, which is compared with data of ref. [17] (open circles) and ref. [18] (closed circles), both taken with 100 eV incident electrons. Representative error bars are indicated.

Some CTMC calculations of doubly-differential cross sections for p and $\bar{p}$ projectiles are shown in figs. 1 and 2. The cross sections in fig. 1 are for 27.2 eV ejected electrons, i.e. for those with velocities half that of the initial projectile velocity ("$v/2$" electrons). Cross sections in fig. 2 are for electrons ejected with the initial projectile velocity ("v" electrons). In fig. 3, we present differential cross sections for $v/2$ electrons with incident electrons and positrons. The zeroth-order physical result of these calculations is that while total ionization cross sections at this energy are fairly similar, the doubly-differential cross sections are enormously different. (Similar effects for these projectiles have been seen in quantum mechanical calculations of double-differential cross sections for 0° electron emission and triply-differential cross sections at larger emission angles [11,12]. Recently, a continuum-distorted-wave calculation has been applied to p and $\bar{p}$ ionization at angles between 0° and 90° [13].) In the extreme case of v electrons created by p and $\bar{p}$ impact, the values can vary by more than three orders of magnitude for ejection angles less than 30°. In all three figures, cross sections for negatively charged projectiles are smaller than those for positively charged ones at small angles, but are larger at the largest angles. The cross section curves intersect each other in all cases at about 60°. The reason for this general behavior can be easily understood classically. We consider a simplistic, but generally appropriate, picture in which target electrons are considered to be bound (i.e., their trajectories are determined by Coulomb attraction to the nucleus) until the projectile has reached its distance of closest approach to the nucleus. At this point, the electron is "ionized", and responds

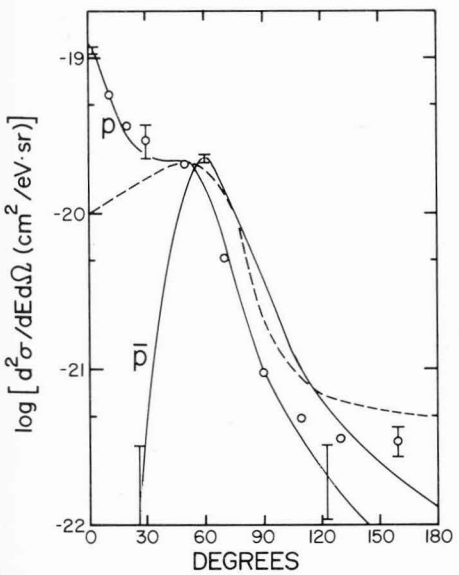

Fig. 2. Doubly-differential cross sections as in fig. 1, but with electron ejection energies of 109 eV. Data designations as in fig. 1.

primarily to the Coulomb force of the projectile. Positive projectiles will tend to pull these free electrons toward them as they exit the collision volume, thereby enhancing emission at small angles. Negative projectiles, on the other hand, will push ejected electrons backward to larger angles of emission.

The prominent sharp rise in the proton cross sections at angles $< 30°$ for v electrons is the well known charge-transfer to-the-continuum cusp. This feature is well described by the CTMC theory, including the asymmetric energy dependence about the projectile velocity [14].

In comparing hadron vs lepton projectiles, we note that at small angles of $v/2$ electron emission (we consider only electrons originating on the target for e^- projectiles), the suppression of cross sections for negative particles is less pronounced in the electron than in the antiproton case: e.g., one and one-half vs three orders of magnitude at 15°. This is another mass effect. During collisions, the light electrons can undergo large deflection and thus fail to inhibit emission at small angles. In contrast, the antiprotons follow straight line trajectories, being scattered to angles less than a few milliradians.

The CTMC calculation can, of course, distinguish between projectile and target electrons. The results of fig. 3 for incident electrons indicate that most of the emitted $v/2$ electrons come from the target. At small angles, however, a majority come from the incident beam, created in close collisions in which a major fraction of the projectile energy is transferred to the target electron.

Shown also in figs. 1–3 are the first Born approximation calculations of Madison [15] for incident protons, and several representative sets of measurements for incident protons [16] and electrons [17,18]. The proton data of Rudd et al. [16] have been multiplied by a factor of 0.777 to yield the revised total cross section of ref. [6]. While the agreement between the CTMC calculations and these data is excellent below 90°, it becomes poor at the largest angles. Recent experimental work at 100 keV has resulted in cross sections which agree fairly well with those of ref. [6] at small angles, but which lie below them at large angles by an amount which would account for most of the discrepancy seen in figs. 1 and 2 [19]. Our calculations can be compared with electron projectile experiments by adding the contributions from the incident beam to the target cross sections. Again we find good overall agreement between experiment and theory, with some discrepancy at the largest scattering angles.

It is clearly desirable to experimentally test these predictions with antimatter projectiles. We consider incident positrons, because the available intensities and energy widths of e^+ beams would appear to make such experiments more feasible at present than those with

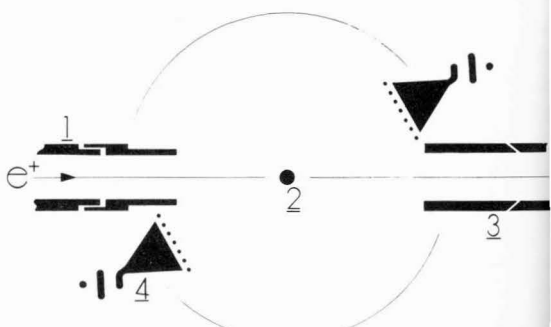

Fig. 4. Schematic diagram of e^+–He collision chamber sho ing 1), final filter lens elements; 2), effusive He target; shielding lens prior to reaccelerator and electrostatic bend; channeltron detector with retarding-field analyzer grid.

antiprotons [2,20]. The schematic diagram for a possib target chamber is shown in fig. 4. Positrons wou emerge from a filter lens and collide with an effusive H beam from a concave glass capillary array. Such arra can produce a focussed target 6 mm in diamet (FWHM) with a density of 10^{14} cm^{-3} [21]. We assun a remoderated positron intensity of 10^7 s^{-1}, current available at Brookhaven National Laboratory [2 Scattered electrons would be detected in two (or fou 2.5 cm mouth channeltrons, located at angles betwe 30° and 150°. These detectors would subtend a sol angle of 0.12 sr each, and would be preceded by negatively-biased grid acting as a retarding fie analyzer. The channeltron cones would be positive

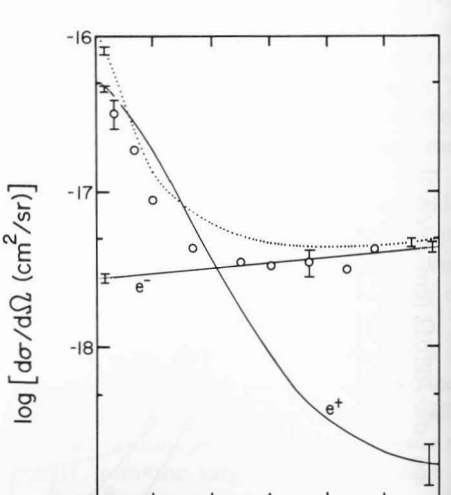

Fig. 5. Singly-differential cross sections for 109 eV incide energy electrons and positron. Cross sections for ejection target electrons are indicated by solid lines; the dotted line the sum of target and beam contributions for incident ele trons, compared with integrated data of ref. [17], taken wi 100 eV incident electrons.

biased to prevent detection of scattered positrons. The primary source of background is expected to be VUV photons, emitted by excited target atoms. Adding the relevant cross sections for He VUV production [7,22] and assuming a VUV detection efficiency of 10%, we obtain background rates between 5 and 10 Hz in each detector. With no bias on the first grid, the signal rates are given by the single-differential angular cross sections, integrated over electron emission energy, shown in fig. 5 [23]. These correspond to 10 Hz at 150°, up to 2 kHz at 30°. (It is important to note that even the singly differential cross sections of fig. 5 show large differences for e^+ and e^- projectiles.) Detailed information about the doubly-differential cross sections can thus be obtained at small angle by differentiating the count-rate vs grid-bias curves. Somewhat cruder information at the larger angles can probably be extracted. In any case, the experiment can test the singly differential calculations quite adequately, which by themselves illustrate clearly the different dynamics of electron and positron ionization.

This work was supported by the DOE (Office of Fusion Energy Grant nos. DOE DE FG02 84ER53175 and 84ER53188) and NSF (Grant no. PHY 8602066).

References

[1] N.F. Mott and N.S.W. Massey, The Theory of Atomic Collisions, 3rd ed. (Oxford University Press, New York, 1987).
[2] L.H. Anderson, P. Hvelplund, H. Knudsen, S.P. Moller and A.H. Sorensen, Phys. Rev. A36 (1987) 3612.
[3] See for example D. Fromme, G. Kruse, W. Raith, and G. Sinapius, Phys. Rev. Lett. 57 (1986) 3031.
[4] See for example, O. Sueoka, J. Phys. Soc. Jpn. 51 (1982) 3757.
[5] See for example, L.M. Diana, L.S. Fornari, S.C. Sharma, P.K. Pendleton, and P.G. Colemen, in: Positron Annihilation, eds. P.C. Jain, R.M. Singru, and K.P. Gopinathan (World Scientific, Singapore, 1985) pp. 342 and 343.
[6] M.E. Rudd, Y.-K. Kim, D.H. Madison, and J.W. Gallagher, Rev. Mod. Phys. 57 (1985) 965.
[7] C.F. Barnett, J.A. Ray, E. Ricci, M.I. Wilker, E.W. McDaniel, E.W. Thomas, and H.B. Gilbody, Atomic Data for Controlled Fusion Research, ORNL Report 5207 (February 1977).
[8] R.E. Olson and A. Salop, Phys. Rev. A16 (1977) 531.
[9] R.E. Olson, J. Phys. B12 (1979) 1843.
[10] J.H. McGuire and L. Weaver, Phys. Rev. A16 (1977) 41.
[11] C.R. Garibotti and J.E. Miraglia, Phys. Rev. A21 (1980) 572.
[12] See for example, P. Mandal, K. Roy, and N.C. Sil, Phys. Rev. A33 (1986) 756;
M. Brauner and J.S. Briggs, J. Phys. B19 (1986) L325.
[13] P.D. Fainstein, V.H. Ponce, and R.D. Rivarola, J. Phys. B21 (1988) 2989.
[14] R.E. Olson, T.J. Gay, H.G. Berry, E.B. Hale, and V.D. Irby, Phys. Rev. Lett. 59 (1987) 36.
[15] D.H. Madison, Phys. Rev. A8 (1973) 2449.
[16] M.E. Rudd, L.H. Toburen, and N. Stolterfoht, At. Data Nucl. Data Tables 18, (1976) 413.
[17] M.E. Rudd and R.D. DuBois, Phys. Rev. A16 (1977) 26; R.D. DuBois, private communication;
see also, for example, R. Müller-Fiedler, K. Jung, and H. Ehrhardt, J. Phys. B19 (1986) 1211 and refs. therein.
[18] C.B. Opal, E.C. Beaty, and W.K. Peterson, At. Data 4 (1972) 209.
[19] D.K. Gibson and I.D. Reid, J. Phys. B19 (1986) 3265.
[20] M. Weber, K.G. Lin, L.O. Roellig, A.P. Mills, Jr., and A.R. Moodenbaugh, in: Atomic Physics with Positrons, ed. J.W. Humberston (Plenum, New York, 1988) in press.
[21] C.B. Lucas, J. Phys. E6 (1973) 991.
[22] C.B. Singh, R. Srivastava, and D.K. Rai, Phys. Rev. A27 (1983) 302.
[23] R.E. Olson and T.J. Gay, Phys. Rev. Lett. 61 (1988) 302.